ICONHIC 2016
1st International Conference on Natural Hazards & Infrastructure
28-30 June, 2016, Chania, Greece

Risk assessment of critical facilities to moderate and extreme seismic events including tsunami. The case of the harbor of Thessaloniki.

K. D. Pitilakis[1], S. A. Argyroudis, S. D. Fotopoulou, S. V. Karafagka, K. G. Kakderi
Aristotle University of Thessaloniki, Greece

J. Selva
Istituto Nazionale di Geofisica e Vulcanologia, Bologna, Italy

ABSTRACT

A new engineering risk based methodology for stress testing of non-nuclear critical infrastructures (CIs) is applied to the port of Thessaloniki in Greece exposed to seismic, geotechnical and tsunami hazards. The methodology workflow consists of four phases: Pre-Assessment, Assessment, Decision and Report phase performed in sequence. In the pre-assessment phase, all the necessary information of the port is archived. The inventory includes buildings, waterfronts, cranes and the electric power supply system. Generic or site-specific fragility models are used for all exposed elements and considered hazards. Risk measures and objectives are defined related to the functionality of the system and the structural losses. In the first level of the assessment phase, the performance of each component is evaluated using a risk-based approach for seismic and tsunami hazards. Then, a system level probabilistic risk analysis is conducted separately for earthquake and tsunami hazards. A scenario-based risk analysis is also carried out focusing on site specific response and extreme seismic events. In the Decision phase, the results of risk assessments are compared with the predefined objectives to decide whether it passes, partly passes or fails the test. This phase also includes guidelines and strategies to improve the performance and resilience of the port.

Keywords: probabilistic risk assessment, scenario-based risk assessment, tsunami, systemic analysis

INTRODUCTION

Critical Infrastructures (CIs) provide the essential services to the society and represent the backbone of economy, security and health. An infrastructure is constituted by an interconnection of assets, therefore the characterization of linkages and overall behavior of the system is a challenging issue. The safety and resiliency of society is a top priority today and is strongly dependent on the resiliency of CIs. In this respect, advanced and standardized tools for hazard and risk assessment of CIs are required, including low-probability high-consequences (LP-HC) events (so-called extreme events) and the systematic application of these new tools to whole classes of critical infrastructures. The European research project STREST: "Harmonized approach to stress tests for critical infrastructures against natural hazards" (www.strest-eu.org), proposed a new engineering risk based multi-level framework for stress tests named ST@STREST for non-nuclear CIs of different classes (Esposito et al. 2017). The methodology is based on a common CI taxonomy and rigorous models for the hazard, vulnerability, performance and resilience assessment under different natural hazards. Different levels of stress tests are proposed, based on the complexity of the analysis (e.g. quantification of epistemic uncertainty, expert elicitation) and the risk assessment approaches (single or multi-hazard, probabilistic or scenario based). A formalized multiple expert integration process has been developed dealing

[1] Corresponding Author: K.D. Pitilakis, *Aristotle University of Thessaloniki, kpitilak@civil.auth.gr*

with the management of epistemic uncertainty called EU@STREST (Epistemic Uncertainty at STREST) (Selva et al. 2015) and integrated into the stress test Workflow (Esposito et al. 2017). The key actors involved in the implementation of the stress test are the Project Manager (PM, representing the stakeholder), the Technical Integrator (TI, an analyst coordinating the assessment), the Evaluation Team (ET, one or more experts implementing the assessment following the Technical Integrator guide), the Pool of Experts (PoE, experts provide input to the TI for making the critical decisions along the process), and the Internal Reviewers (IR, one or more experts performing a participatory review). All these actors should interact along the stress test to assure the robustness of stress test results, considering the potential limitation in the available budget for non-nuclear critical infrastructures.

The core idea implemented in ST@STREST is to develop a methodology which evaluates the performance of a CI to single or multiple hazards by comparing specific risk objectives related to the functionality of the CI as a whole, the port system in this case, and the structural losses at component level, with the results of a risk based assessment at component level for the acceptable probability of collapse (typically implied by the codes) and at a second stage with a system level full probabilistic risk analysis considering specific interdependencies between networks and components.

ST@STREST is applied and tested in six critical infrastructures in Europe (Pitilakis et al. 2016). The port of Thessaloniki, one of the most important ports in Southeast Europe and the largest transit-trade port in Greece, is one of the case studies, a characteristic example of distributed and/or geographically extended infrastructures with potentially high economic and environmental impact. The port occupies a total space of 1.5 million m^2, includes 6 piers spreading on a 6200 m long quay and a sea depth down to 12 m, with open and indoors storage areas, suitable for servicing all types of cargo and passenger traffic. The port also has installations for liquid fuel storage, while is located in proximity to the international natural-gas pipeline and is linked to the national and international road and railway network (www.thpa.gr).

The goal of this study is to apply the ST@STREST framework to the port infrastructures exposed to different seismic hazards i.e. ground shaking, liquefaction and tsunami. The framework consists of four phases: Pre-Assessment, Assessment, Decision and Report phase, which are performed in sequence. Each phase is subdivided in a number of specific steps as described in Fig. 1.

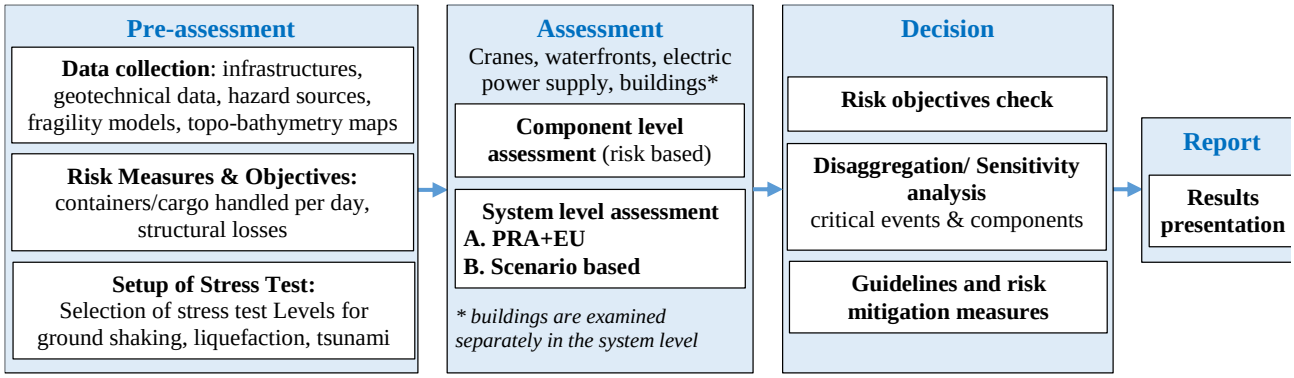

Figure 1. Flowchart of the ST@STREST framework for the stress test application in the port of Thessaloniki

Phase 1 Pre-Assessment: In the pre-assessment phase all the necessary data is collected and archived in a GIS database. The inventory includes port facilities, various buildings, quay walls, cranes and networks (e.g. electric power supply system). The vulnerability of the infrastructures to the given target hazards (i.e. ground shaking, liquefaction, and tsunami) is assessed using site and case specific or generic fragility functions. Specific risk metrics and objectives are defined related to the functionality of the port system and the structural losses. The stress test levels are selected and the accuracy of the adopted methods in the stress test is defined according to ST@STREST framework.
Phase 2 Assessment: The assessment phase comprises two distinctive steps: the component level assessment and the system level assessment (probabilistic or scenario based). *In the first one*, a risk-based assessment of each component is carried out for earthquake and tsunami hazards to check whether the component passes or fails the minimum requirements for its performance. For that, the target (acceptable) probability of collapse implied by the code, stakeholders and decision-makers needs should be pre-defined for each component. Then

in the second step, a probabilistic risk analysis (PRA) is conducted for the whole system separately for earthquake and tsunami hazards considering specific interdependencies between network and components. In addition, at this second step, a scenario-based risk analysis (SBRA) is also performed focusing on site specific response and extreme seismic events.
Phase 3 Decision: The estimated response is compared with predefined acceptable risk criteria in order to assess the performance of the CI and decide whether it passes, partly passes or fails the test for all possible events and to define how much the safety of the CI should be improved until the next periodical verification (Esposito et al. 2017). The decision phase also includes disaggregation and sensitivity analysis for the identification of the critical components and events, guidelines and strategies to improve the performance and the resilience of the port as a critical facility.
Phase 4 Report: This ultimate phase includes presentation of the outcome of the stress test to the port Authority.

PRE-ASSESSMENT PHASE

Data collection

A GIS database for the port facilities was developed by the Research Unit of Soil Dynamics and Geotechnical Earthquake Engineering (SDGEE, sdgee.civil.auth.gr) at Aristotle University of Thessaloniki in collaboration with the port Authority in the framework of previous national and European projects and it is further updated in STREST project (www.strest-eu.org). Waterfront structures, cargo handling equipment, buildings (offices, sheds, warehouses etc.) and the electric power supply system are examined (Fig. 2). The SYNER-G (www.syner-g.eu, Pitilakis et al. 2014a) taxonomy is used to describe the different typologies. Waterfront structures include concrete gravity block type quay walls with simple surface foundation and non-anchored components. Cargo handling equipment has non-anchored components without backup power supply. Four gantry cranes are used for container loading-unloading services located in the western part of the 6th pier. The electric power supply to the cranes is assumed to be provided through non-vulnerable lines from the distribution substations that are present inside the port facilities. They are classified as low-voltage substations, with non-anchored components. In total, 85 building and storage facilities are considered in the analyses. The majority is reinforced concrete (RC) buildings comprising principally of low- and mid-rise infilled frame and dual systems with low or no seismic design. The steel buildings are basically warehouses with one or two floors while the unreinforced masonry (URM) buildings are old low-rise and mid-rise structures.

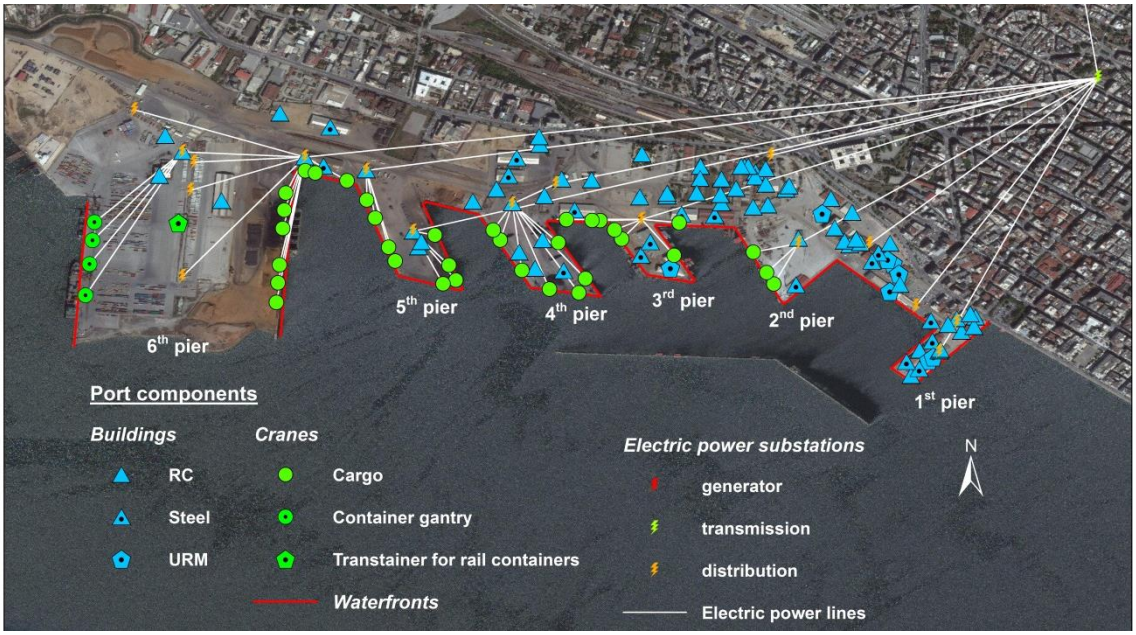

Figure 2. Geographical representation of Thessaloniki's port infrastructures considered in the study

Soft alluvial deposits, sometimes susceptible to liquefaction, characterize the Port subsoil conditions. The thickness of these deposits close to the sea may reach 150 m to 180 m. A comprehensive set of in-situ geotechnical tests (e.g. drillings, sampling, SPT and CPT tests), detailed laboratory tests and measurements,

as well as geophysical surveys (cross-hole, down-hole, array microtremor measurements) at the port broader area provide all necessary information to perform any kind of site specific ground response analyses (Anastasiadis et al., 2001). Complementary geophysical tests including array microtremor measurements have been conducted in the frame of STREST project at four different sites inside the port (Pitilakis et al., 2016) using the SPatial Autocorrelation Coefficient–SPAC method (Aki, 1957). All available data (Fig. 3) are properly archived. A topobathymetric model was also produced for the tsunami simulations, based on nautical and topographic maps and satellite images (Fig. 4). The elevation data includes also the buildings and other structures that affect the waves while propagating inland. The resolution of the model is higher in the area of the Port.

Figure 3. Location of geotechnical tests and geophysical field measurements in Thessaloniki's port area

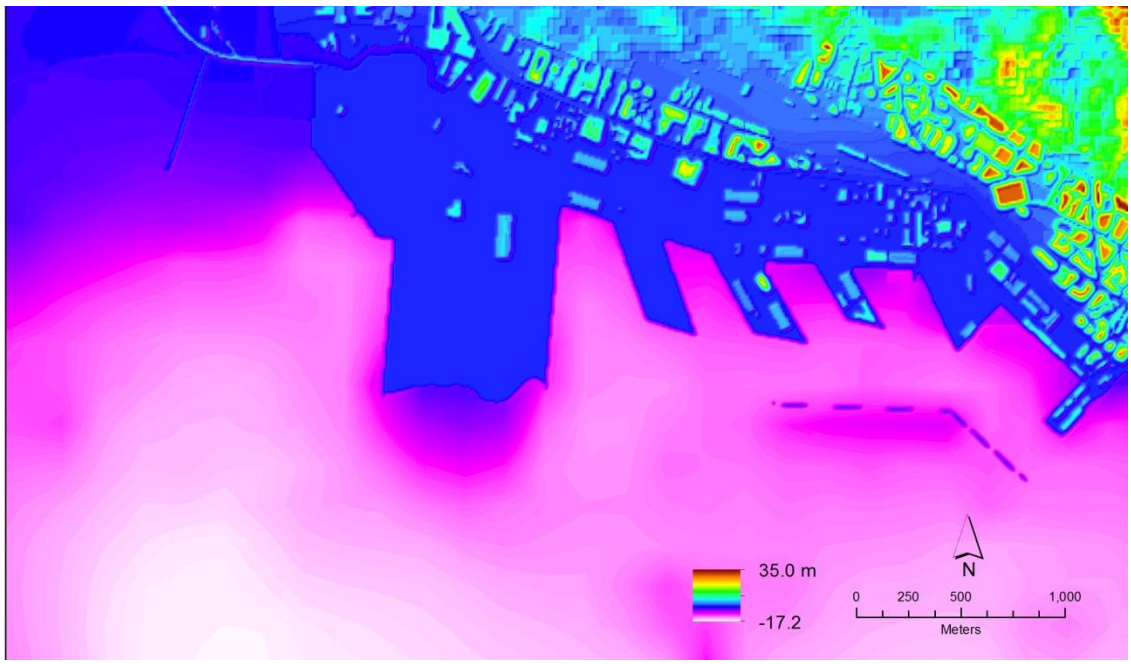

Figure 4. Digital elevation map of Thessaloniki's port area

Fragility models

The vulnerability of the Port facilities at component level (i.e. buildings, waterfront structures, cranes etc) is assessed through fragility functions (Pitilakis et al. 2014a), which describe the probability of exceeding predefined damage states (DS) for given levels of peak ground acceleration (PGA), permanent ground displacement (PGD) and inundation depth for the ground shaking, liquefaction and tsunami hazards respectively (Table 1). The fragility functions used to assess the damages due to liquefaction are generic (NIBS, 2004), while the models used for ground shaking are either case specific (UPGRADE, 2015; Kappos et al. 2003, 2006; SRM-LIFE 2007, present work) or generic (NIBS, 2004).

New seismic fragility curves have been developed for typical quay walls and gantry cranes of the port subjected to ground shaking based on dynamic numerical analyses in collaboration with the National Technical University of Athens (NTUA) (UPGRADE, 2015). The model included the quay wall blocks, the surrounding soil and the embankment, as well as concentrated gravity loads on the position of container crane legs and a uniform operational load on the embankment (Kourkoulis et al, 2014). Twelve seismic motions are selected in the analyses to account for seismic scenarios of moderate and high seismicity scaled up to different amplitudes (up to ± 0.3g) and applied at the model base through viscous dampers. Then, for each seismic analysis, the engineering demand parameter (EDP) is estimated. In particular, the ratio of the residual displacement (towards the sea) at the top of the wall (u_x) to the height of the quay wall (H) is considered as EDP (u_x/H) for the quay wall, while the resultant (horizontal and vertical) residual differential displacement of the crane legs (du) is taken as EDP for the crane. Finally, lognormal distribution functions are established as a function of the peak ground acceleration (PGA) at free field conditions to represent the fragility curves for predefined damage states (according to PIANC 2001 and NIBS 2004 for the quay wall and the crane respectively). Fig. 5 illustrates the fragility curves and its parameters (i.e. median m and log- standard deviation beta) for the quay wall and the crane.

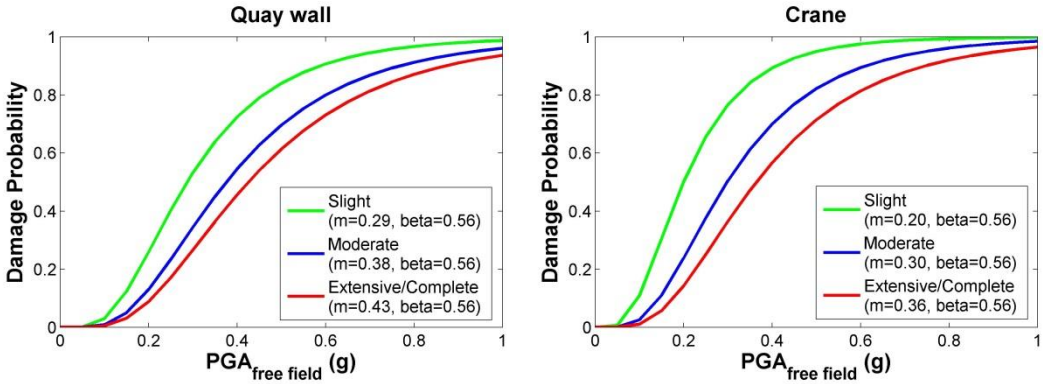

Figure 5. Fragility curves for the quay wall (left) and the crane (right) for ground shaking

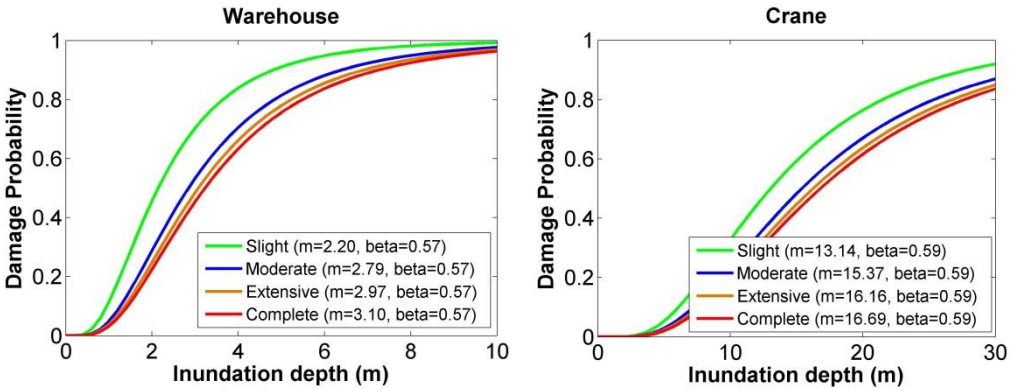

Figure 6. Tsunami fragility curves for the warehouse (left) and the crane (right)

Analytical tsunami fragility curves as a function of inundation depth have been developed for representative typologies of the Port RC buildings, warehouses and gantry cranes (Karafagka et al., 2016; Salzano et al., 2015) while, for simplicity reasons, the waterfront structures are considered as non-vulnerable to tsunami

forces. An extensive numerical parametric investigation has been performed considering different combinations of statically applied tsunami loads based on FEMA (2008) recommendations for gradually increasing tsunami inundation depths. Afterwards, the structure's response in terms of material strain (i.e the EDP) for the different statically applied tsunami loads is estimated. For the development of fragility curves, a relationship between the numerically calculated material strain (i.e. the EDP) and the gradually increasing inundation depths (i.e. the IM) is established through nonlinear regression analysis. Indicatively, the tsunami fragility curves for warehouses and cranes are presented in Fig. 6.

The damage states are correlated with component functionality in order to perform the risk assessments in the system level. The following assumptions are set: (i) the waterfront-pier (berth) is functional if damage is lower than moderate, (ii) the crane is functional if damage is lower than moderate and there is electric power supply (i.e. the physical damages of the substations are lower than moderate) (iii) the berth is functional if the waterfront and at least one crane is functional.

Table 1. Fragility functions used in the risk analyses

Hazard	Component	Intensity measure	Reference
Ground shaking	RC and URM buildings	PGA	Kappos et al. (2003, 2006)
	Steel buildings		HAZUS (NIBS, 2004)
	Waterfront structures		UPGRADE (2015) - Fig. 5
	Cranes/cargo handling equipment		
	Electric power substations (distribution, transmission)		HAZUS (NIBS, 2004), SRM-LIFE (2003-2007)
Liquefaction	Buildings/ Housed electric power substations (all considered typologies)	PGD	HAZUS (NIBS, 2004)
	Waterfront structures		
	Cranes/cargo handling equipment		
Tsunami	RC Buildings/ Electric power substations	Inundation depth	Karafagka et al. (2016)- Fig. 6
	Warehouses (Steel and URM buildings)		Salzano et al. (2015)
	Cranes/cargo handling equipment		

Definition of risk metrics and objectives

In the Pre-Assessment phase, specific risk measures and objectives are defined related to the functionality of the port at system level and the structural losses at component level. Since two terminals (container, bulk cargo) are assumed herein, the system performance is measured through the total number of containers handled (loaded and unloaded) per day (TCoH), in Twenty-foot Equivalent Units (TEU), and the total cargo handled (loaded and unloaded) per day (TCaH), in tones. Risk measures related to structural and economic losses of the buildings are also set for the tsunami case and the scenario based assessment. The risk objectives correspond to the boundaries of the grading system proposed in ST@STREST (Esposito et al. 2017). The CI passes the stress test if is classified into grade AA (negligible risk) or A (risk being as low as reasonably practicable, ALARP). The CI partly passes the stress test if it receives grade B (possibly unjustifiable risk), while it fails the stress test if it is classified into grade C (intolerable risk). Since no regulatory boundaries exist for the moment for port facilities, continuous (i.e. straight lines on the logarithmic performance curve, see Figs. 7 and 8) and scalar (i.e. expected performance loss, see Table 3) boundaries were defined based on general judgment criteria for the probabilistic and scenario based system-wide risk assessment respectively in order to demonstrate the application of the ST@STREST. The stress test levels are defined and outlined in the following section.

ASSESSMENT PHASE

Component level assessment

The aim is to check each component of the port independently for earthquake and tsunami hazards in order to show whether the component passes or fails the pre-defined minimum requirements for its performance implied by the current codes. A risk-based assessment is performed using the hazard function at the location of the component and the fragility function of the component. These two functions are convolved in risk integral in order to obtain probability of exceedance of a designated limit state in a period of time (P_f). This probability is estimated on the basis of closed form risk equation (Fajfar and Dolšek, 2012) as follows:

$$P_f = \mathrm{H}(\overline{IM})\ \exp(0.5\,\mathrm{k}^2\beta^2) \quad (1)$$

where $\overline{IM}$ and β are the median and log-standard deviation values respectively of the fragility function, H(IM) is the hazard function and k is the logarithmic slope of the hazard function idealized in the following form:

$$\mathrm{H(IM)} = \mathrm{k_o}\cdot\mathrm{IM}^{-\mathrm{k}} \quad (2)$$

where k_o is a constant that depends on the seismicity of the site. Proper k and k_o can be obtained by fitting the actual hazard curve provided that the entire hazard function or at least two points from the hazard function are available. For the seismic case (i.e. ground shaking), k and k_o were computed from the hazard curve corresponding to return periods equal to 475 and 4975 years for the normal and the extreme event respectively based on the site specific response analyses carried out for three representative soil profiles (scenario-based assessment) (e.g. Fig. 7- left). For the tsunami case, at least two points of the mean hazard function estimated from probabilistic tsunami hazard assessment at various locations in the port area were used to estimate these parameters (e.g. Fig. 7- right). The target (acceptable) probability of exceedance of a designated limit state for a period of time implied by the code, stakeholders and decision makers (P_t) also has to be defined for each component and different limit states. In this application the target probability of exceedance of the collapse damage state is only provided. This probability was set to $1.0\cdot10^{-5}$ based on the existing practice (e.g. Lazar and Dolšek 2013; Silva et al. 2014) corresponding to an acceptable probability equal to 0.05% in 50 years and was properly modified based on EC8 prescriptions to account for the importance factor γ_I of the structure. To check whether or not the component is safe against collapse, the target probability (P_t) is compared with the corresponding probability of exceeding the ultimate damage state (P_f).

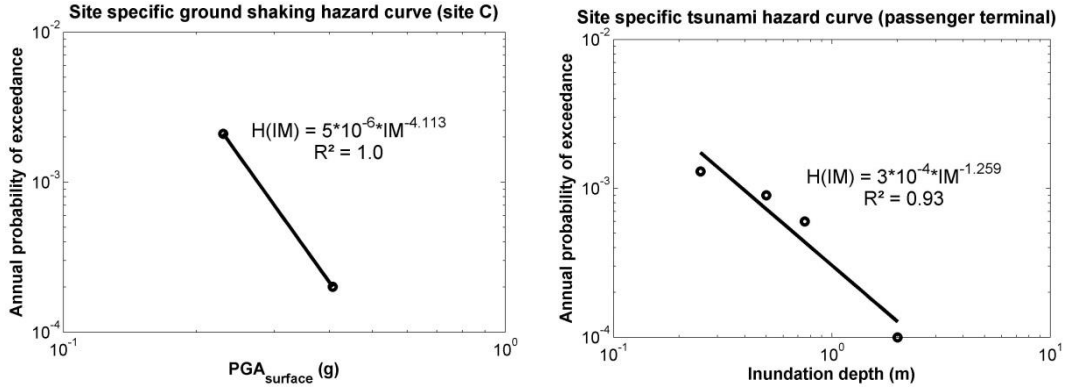

Figure 7. Site specific hazard curves for ground shaking and tsunami

As an example the proposed performance assessment approach is applied here to a strategic building of the Port, the passenger terminal, which is a low-rise infilled dual system (γ_I =1.2). The probability of exceeding the ultimate damage state (P_f), which in this study corresponds to the collapse damage state, is computed and compared with the target probability of collapse (P_t) for both earthquake and tsunami hazards. The hazard function at the location of the structure is estimated as 10^{-5} and $1.7\cdot10^{-4}$ for the seismic (see Fig. 7- left and Equation 2) and tsunami (see Fig. 7- right and Equation 2) case respectively, while the corresponding probabilities of collapse (P_f) are finally computed equal to $1.4\cdot10^{-3}$ and $2.0\cdot10^{-4}$. These probabilities are higher than the target (acceptable) probability of collapse (P_t) estimated equal to $4.7\cdot10^{-6}$ and $7.9\cdot10^{-6}$ for the seismic and tsunami case respectively, indicating that the structure is not safe against exceedance of the collapse limit

state due to the considered hazards. Similar results are generally derived for all buildings and infrastructures providing a general assessment of the performance and resilience of the Port.

System level assessment

a) Probabilistic risk assessment (PRA)

The system wide probabilistic risk assessment is made separately for ground shaking, including liquefaction, and tsunami hazard, according to the methodology developed in SYNER-G (Pitilakis et al. 2014b) and extended in STREST (Kakderi et al. 2015). The objective is to evaluate the probability or mean annual frequency (MAF) of events with the corresponding loss in the performance of the port operations. The analysis is based on an object-oriented paradigm where the system is described through a set of classes, characterized in terms of attributes and methods, interacting with each other. The physical model starts from a pre-defined taxonomy and requires: a) a description of the functioning of the system (intra-dependencies) under undisturbed and disturbed conditions (i.e., in the damaged state following an event); b) a model for the physical and functional damageability of each component (fragility functions); c) identification of all dependencies between systems (inter-dependencies); and d) definition of adequate Performance Indicators (PIs) for components and the system as a whole which represent the previously defined risk metrics. The computational modules include the modelling of: hazard events and intensity parameters (hazard class), physical damages of components and performance of the system (network class), and specific interactions among systems (interdependency models). A Monte Carlo simulation is carried out sampling events and corresponding damages for the given hazard. The exceedance probability of different levels of performance loss is assessed for the system under the effect of any possible event, and the performance curve is produced, which is equivalent of risk curves for non-systemic probabilistic assessments in single (e.g. PEER formula, Cornell and Krawinkler, 2000) and/or multi-risk (e.g. Selva, 2013) analysis.

In the present application the systemic analysis concerns the container and bulk cargo movements affected by the performance of the piers, berths, waterfront and container/cargo handling equipment (cranes) while the interdependency considered here is between the cargo handling equipment and the Electric Power Network (EPN) supplying to cranes. The capacity of berths is related to the capacity of cranes (lifts per hour/tons per hour). The functionality state of each component and the whole port system is assessed based on the computed physical damages, taking also into account system inter- and intra-dependencies. Regarding the analysis of the interdependencies we assume that if a crane node is not fed by the reference EPN node (i.e. electric supply station) with power and the crane does not have a back-up supply, then the crane itself is considered out of service. The functionality of the demand node is based on EPN connectivity analysis (Pitilakis et al. 2014b).

Risk assessment for ground shaking

The seismic hazard model provides the means for: (i) sampling events in terms of location (epicentre), magnitude and faulting type according to the seismicity of the study region and (ii) maps of sampled correlated seismic intensities at the sites of the vulnerable components in the infrastructure ('shakefields' method, Weatherill et al., 2014). When the fragility of components is expressed with different IMs, the model assesses them consistently. Five seismic zones with M_{min}=5.5 and M_{max}=7.5 are selected based on the results of SHARE European research project (Giardini et al., 2013, www.share-eu.org) and the ground motion prediction equation (GMPE) of Akkar and Bommer (2010) to estimate the outcrop ground motion parameters. Seismic events are sampled for the seismic zones affecting the port area through a Monte Carlo simulation (10,000 runs). The spatial variability is modelled using the correlation models provided by Jayaram and Baker (2009). For each site of a regular grid of points discretizing the study area, the averages of primary IM (PGA) from the specified GMPE were calculated, and the residual was sampled from a random field of spatially correlated Gaussian variables according to the spatial correlation model. The primary IM is then retrieved at vulnerable sites by distance-based interpolation and finally the local IM is sampled conditionally on primary IM. Fig. 8 shows an example map with the primary IM (PGA at rock) computed at points of a regular grid, for a sampled event corresponding to a return period of 500 years, modeling the spatial variability of the ground motion. To scale the hazard to the site condition the amplification factors proposed in EC8 (EN 1998-1, 2004) are used in accordance with the site classes that were defined in the study area. HAZUS (NIBS, 2004) and the modelling

procedure by Weatherill et al. (2014) are applied to estimate the permanent ground displacements (PGDs) due to liquefaction.

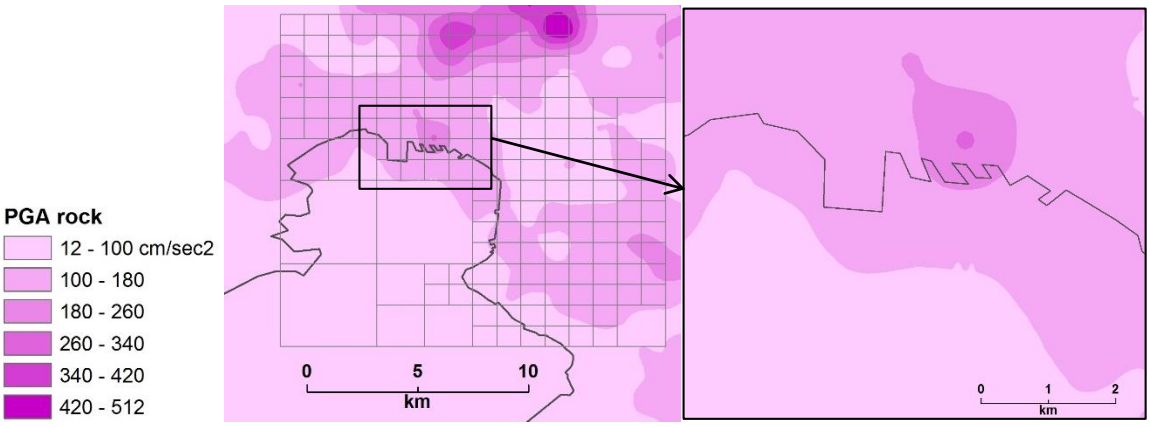

Figure 8. Example of shake map in terms of PGA on rock for one event (M =5.8, R =20 km NNE of Port).

The PIs of the port system for both the container and cargo terminal are evaluated for each simulation of the Monte Carlo analysis based on the damages and corresponding functionality states of each component and considering the interdependencies between components. The final computed PIs are normalized to the value referring to normal (non-seismic) conditions assuming that all cranes are working at their full capacity 24 hours per day. Fig. 9 shows the MAF of exceedance curves ("performance curve") for TCoH and TCaH. For performance loss values below 40% TCaH yields higher values of exceedance frequency, while for performance loss over 40% TCoH yields higher values of exceedance frequency.

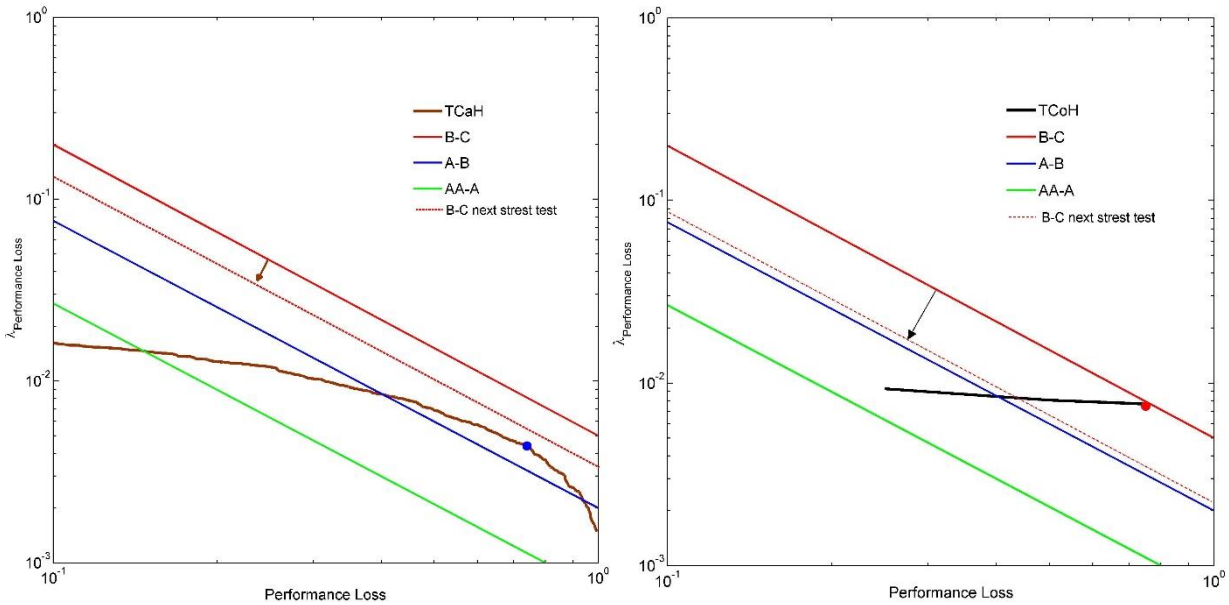

Figure 9. Mean annual frequency (MAF) of exceedance values for the normalized performance loss of the container terminal (TCoH, right) and the bulk cargo terminal (TCaH, left) for the seismic hazard case. The green, blue and red continuous lines correspond to the boundaries between risk grades AA (negligible), A (ALARP), B (possibly unjustifiable risk), and C (intolerable).

Risk assessment for tsunami

A full SPTHA (Seismic Probability Tsunami Hazard Analysis) for tsunami of seismic origin, following Lorito et al. 2015) has been developed, based on inundation simulation of the Thessaloniki area (Volpe et al. in prep). Different potential tsunamigenic sources should be considered, such as earthquakes, landslides, meteorite impacts or atmospheric phenomena. Here, we focus only on tsunami of seismic origin, which is in most of cases the dominant component (Parsons and Geist, 2009). A very large number of numerical simulations of

tsunami generation, propagation and inundation on high resolution topo-bathymetric models are in principle required, in order to give a robust evaluation of SPTHA at a local site. To reduce the computational cost, while keeping results stable and consistent with respect to explore the full variability of the sources, a method has been developed to approach the uncertainty in SPTHA (Volpe et al., in prep; Selva et al. 2016a, 2016b), based on four steps: 1) a full exploration of the aleatory uncertainty through an Event Tree (ET, Lorito et al. 2015, Selva et al. 2016a) that accounts for all available sources of information (e.g., Basili et al. 2013); 2) the propagation of all potential sources till off-shore (Molinari et al., submitted); 3) a 2-stage filtering procedure based on Cluster Analysis on the results off-shore in order to define a sub-set of "representative" events which approximate the hazard in the target area, in order to enable the inundation modelling (Lorito et al. 2015); 4) the quantification of the epistemic uncertainty through Ensemble modelling based on (weighted) alternative implementations of steps 1 to 3 (Marzocchi et al. 2015; Selva et al. 2016a).

For Thessaloniki port (Selva et al. 2016b; Volpe et al., in prep), at steps 1 and 2, we considered a regional SPTHA which accounts for all the potential seismic sources from the Mediterranean Sea (>107 sources), implementing a large number of alternative models to explore the epistemic uncertainty (>105). Then, the 2-layer filtering procedure has been applied, obtaining 253 representative scenarios which may be modeled to approximate the total hazard (Lorito et al. 2015; Volpe et al., in prep). The numerical simulations were performed using a non-linear shallow-water multi-GPU code (HySEA, Gonzalez Vida et al., 2015), using 4-level nested bathymetric grids with refinement ratio equal to 4 and increasing resolution from 0.4 arc-min (~740 m) to 0.1 arc-min (~185 m) to 0.025 arc-min (~46 m) to 0.00625 arc-min (~11 m). The results have been input to an Ensemble model, in order to quantify in each point of the finest grid hazard curves, along with epistemic uncertainty, for two intensity measures: maximum flow depth and maximum momentum flux.

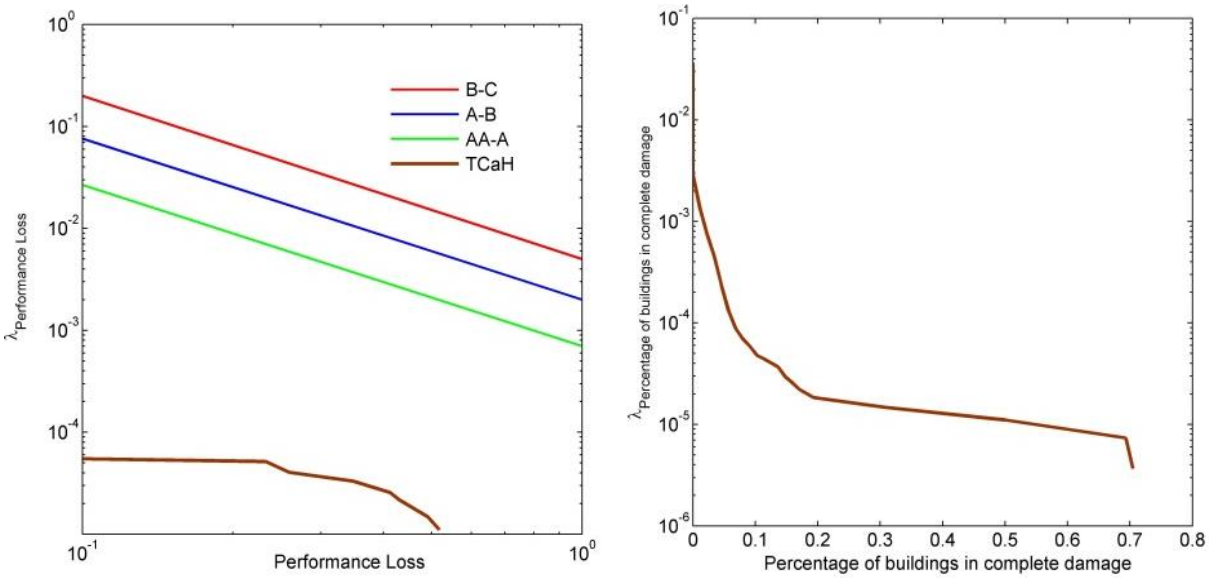

Figure 10. Mean annual frequency (MAF) of exceedance values for the normalized performance loss of the bulk cargo terminal (TCaH, left) and for the buildings in complete damage state (right) for the tsunami hazard case. The green, blue and red continuous lines correspond to the boundaries between risk grades AA (negligible), A (ALARP), B (possibly unjustifiable risk), and C (intolerable).

To assess the tsunami risk a hazard module has been developed in order to enable sampling among the 253 representative scenarios, considering the probability of occurrence of the cluster of sources that each scenario represents (Lorito et al. 2015). This procedure is possible for any preselected alternative model of input to the SPTHA ensemble, enabling the propagation of hazard epistemic uncertainty into risk analysis. The inundation simulation results for each sampled scenario are then loaded, in order to retrieve the tsunami intensity for any selected location. Note that, since the SPTHA analysis is based on an explicit simulation of each scenario, spatial correlations of the tsunami intensity are automatically accounted for. Given that the inundation simulation does not integrate potential collapses, tsunami intensity should be retrieved in proximity of each component's perimeter and outside the structure. In order to avoid any unwanted biases (e.g., retrieve the tsunami intensity over the roof of buildings, where the modelled tsunami flow depth is subtracted the height of the building), a characteristic radius has been assigned to each component, and the largest intensity value

within the defined circle is obtained. Damages and non-functionalities are then sampled from the respective fragility curves (Table 1) and the retrieved tsunami intensities. The analysis has been implemented for the port infrastructures (cranes, electric power network components and individual buildings) and the PIs for the analyzed system are evaluated. In Fig. 10 we show an indicative example for one of the alternative models (i.e. the epistemic uncertainty is not considered here). The container terminal is not expected to experience any loss (TCoH), while the loss in the cargo terminal (TCoH) is negligible. This is due to the non-vulnerable condition of waterfront structures, the high damage thresholds for the cranes (i.e. high inundation values that are not expected in the study area) as described in the fragility curves used in the application and the distance of the electric power substations from the shoreline. The annual probabilities for buildings collapses are also low. As an example 10% of the total buildings in the Port (~9 structures) will be completed damaged under tsunami forces with annual probability equal to $5 \cdot 10^{-5}$.

b) Scenario-based risk assessment

A scenario-based system-wide seismic risk analysis is performed complementary to the classical PRA approach described previously, to identify as accurately as possible the local site response at the port area and to reduce the corresponding uncertainties. Two different seismic scenarios were defined in collaboration with a pool of experts: the standard seismic design scenario and an extreme scenario corresponding to return periods of T_m=475 years and T_m=4975 years respectively. To perform the site response analyses a target spectrum for seismic bedrock conditions (Vs=700-800 m/s) and a suite of acceleration time histories are needed. For the 475 years scenario, the target spectrum is defined based on the disaggregation of the probabilistic seismic hazard analysis (SRM-LIFE, 2007; Papaioannou, 2004). This study has shown that the most significant contribution to seismic hazard for Thessaloniki port is associated with the Anthemountas fault system (i.e. a normal fault) regardless of the return period. In particular, for the 475 years scenario, the maximum annual exceedance probability for a certain PGA value with a moment magnitude M_w of 5.7 and an epicentral distance R_{epi} of 14.6 km was provided. For the 4975 years scenario, an extreme rupture scenario breaking along the whole Anthemountas fault zone with a characteristic magnitude M_w of 7.0, close to the maximum magnitude of the seismic source, was assumed. The GMPE proposed by Akkar and Bommer (2010) is applied, similarly to the probabilistic assessment. In addition to magnitude and distance, both hazard scenarios include an error term ε (which measures the number of standard deviations of logarithmic residuals σ to be accounted for in GMPE) responsible for an appreciable proportion of spectral ordinates and the contribution from ε grows with the return period (Bommer and Acavedo, 2004). Thus, the median spectral values plus 0.5 standard deviations and 1 standard deviation are considered for the 475 years and the 4975 years scenarios respectively. A set of 15 accelerograms is selected for the 475 years scenario referring to rock or very stiff soils that on average fit the target spectrum. For the extreme scenario, 10 synthetic accelerograms are computed to fit the target spectrum (4975 years scenario I) and broadband ground motions are generated using 3D physics-based "source-to-site" numerical simulations (4975 years scenario II, Smerzini et al., submitted).

Three representative soil profiles (denoted as A, B and C) are considered for the site response analyses (see Fig. 3) with fundamental periods T_o equal to 1.58s, 1.60s and 1.24s respectively. The soil profiles have been defined based on previous studies and new measurements. 1D equivalent-linear (EQL) and nonlinear (NL) site response analyses including also the potential for liquefaction are carried out for the three soil profiles using as input motions at the seismic bedrock the ones estimated for the 475 years and 4975 years seismic scenarios (I and II). The numerical codes Strata (Kottke and Rathje 2008) and Cyclic1D (Elgamal et al. 2015) are used. All models assume vertical propagating SH waves from the bedrock to the surface. To investigate the impact of the uncertainty in the shear wave velocity (Vs) profiles, the analyses are performed for the basic geotechnical models, considering a standard deviation of the natural logarithm of the Vs equal to 0.2. In particular, 100 realizations of the Vs profiles are considered in Strata using Monte Carlo simulations and the calculated response from each realization is then used to estimate statistical properties of the seismic response. In total 1500 and 1200 simulations are performed for the 475 and 4975 (I and II) scenarios respectively. The randomization of the Vs and the incorporation in Monte Carlo simulations is performed through the model proposed by Toro (1995). The corresponding site response variability was assessed in Cyclic1D considering expect for the basic Vs model, upper-range and lower-range models utilizing a logarithmic standard deviation for the Vs profile equal to 0.2 consistently with the Strata simulations. For the EQL approach the results are presented in terms of PGA with depth, acceleration response spectra and spectral and fourier ratios. For the NL approach, the variation of horizontal and vertical

PGD, maximum shear strain and stress, effective confinement and excess pore water pressure with depth were also computed for each analysis. Comparative plots between the EQL and NL approaches are shown in Fig. 11 for the 475 years and 4975 years I scenarios for profile A while Fig. 12 depicts indicative results of the NL analysis for the selected input motions for the same soil profile.

The spectral values and shapes are generally well compared between the two approaches for the 475 year scenario while the response is very different for the extreme scenario that is associated with increasing shear strain accumulation. For both scenarios, the EQL spectral shapes are flatter and have less period-to-period fluctuations than the NL ones. The lower spectral values predicted by the NL approach for the extreme seismic scenario could be attributed to the liquefaction that may also result in large permanent ground deformations, which cannot be simulated by the EQL analysis. The results of the NL approach indicate (although not fully presented herein) that liquefaction is evident for all soil profiles and scenarios. However, for the extreme scenario the liquefiable layers are larger and extended to greater depths (up to 35m, e.g. see Fig. 12 -left). Among the three representative soil profiles, liquefaction effects are shown to be more pronounced in profile A. Large variability in the computed permanent displacements is shown for the different seismic input motions (e.g. see Fig. 12 -right). Generally low-frequency input motions increase the accumulation of lateral deformations and settlements. The computed maximum horizontal displacement values when considering the basic geotechnical models are 4.5 cm and 18.6 cm for the 475 and 4975 years seismic scenarios respectively, while the corresponding values for the vertical displacements (settlements) are 4.8 cm and 11.0 cm.

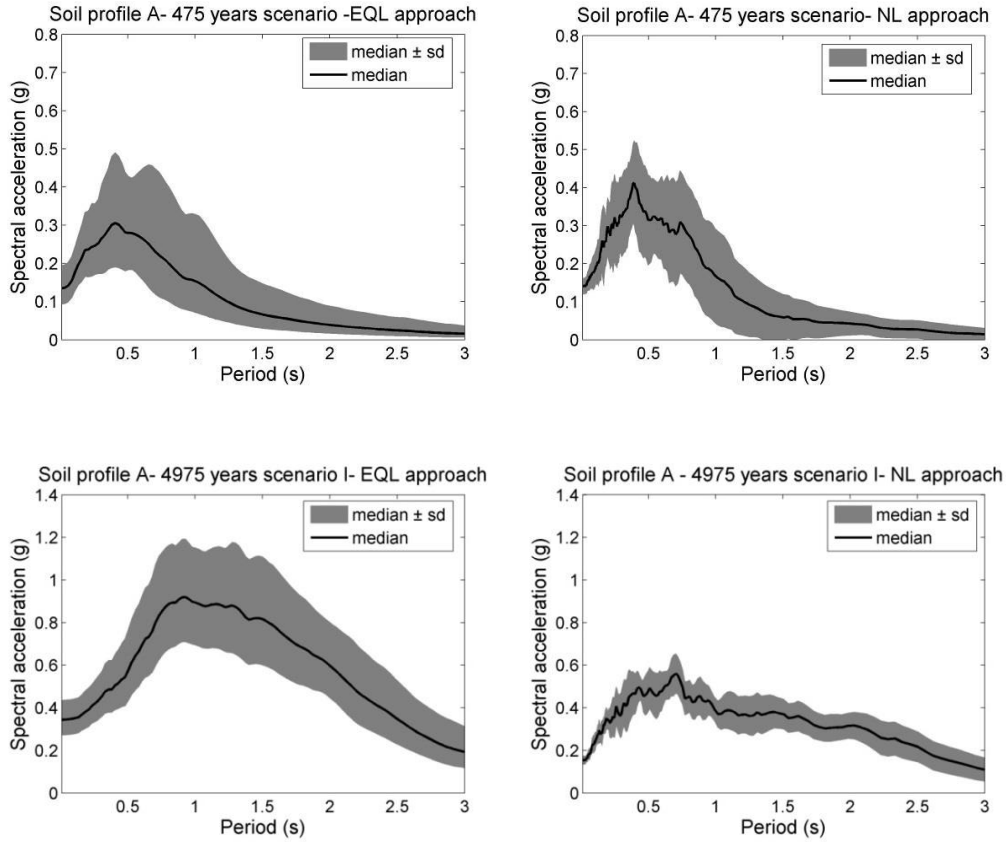

Figure 11. Median ± standard deviation elastic 5% response spectra at the ground surface for soil profile A using the EQL (left) and NL (right) approaches for the 475 years scenario (top) and the 4975 years scenario I (bottom).

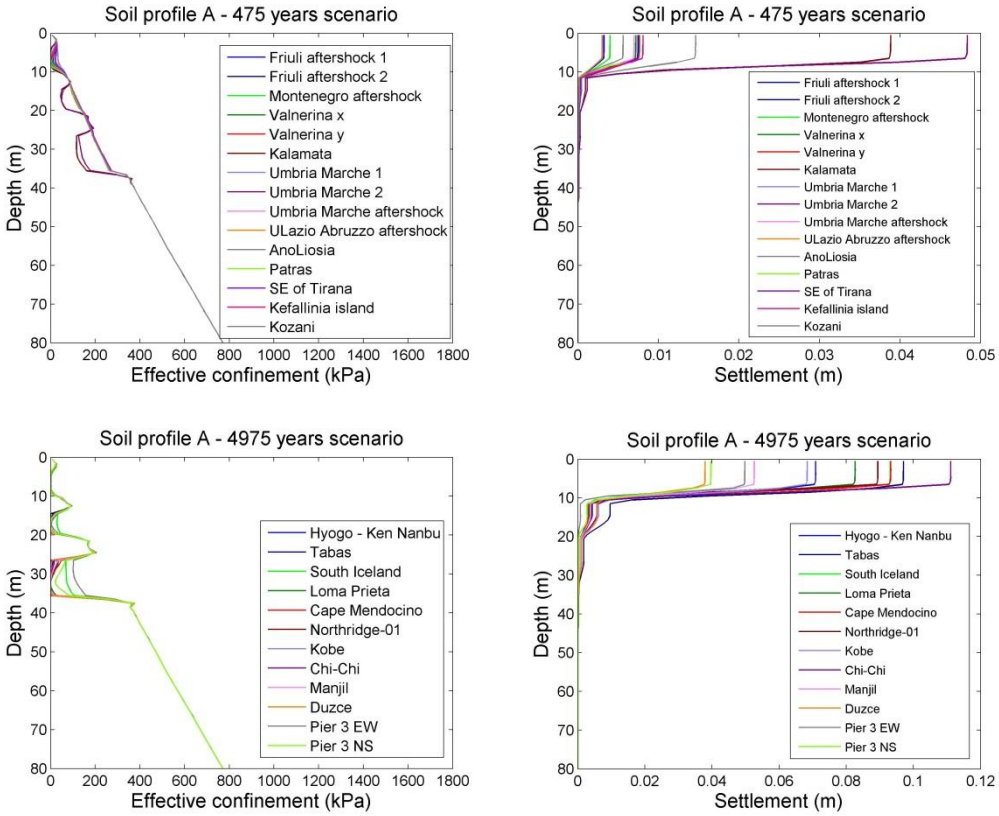

Figure 12. Variation of effective confinement (left) and settlement with depth (right) for soil profile A for the 475 years scenario (top) and the 4975 years scenario (bottom).

The scenario-based risk assessment of the port buildings and infrastructures is initially performed taking into account the potential physical damages and corresponding losses of the different components of the port. Buildings, waterfront structures, cargo handling equipment and the power supply system are examined using the fragility models for ground shaking and liquefaction (Table 1). In particular, the vulnerability assessment is performed for the 475 and 4975 years scenarios (I and II) based on the EQL and NL site-response analyses. The results from soil profile A, B or C were considered in the fragility analysis, depending on the proximity of each component to the location of the three soil profiles. In particular, for the EQL approach, the calculated PGA values at the ground surface from the total analysis cases (i.e. 2200 analyses) for each soil profile were taken into account for the vulnerability assessment due to ground shaking. For the NL approach, except for the PGA values, the PGD (horizontal and vertical) values at the ground surface were also considered to evaluate the potential damages to buildings and infrastructures due to liquefaction effects. Finally, the combined damages are estimated by combining the damage state probabilities due to the liquefaction (P_L) and ground shaking (P_{GS}), based on the assumption that damage due to ground shaking is independent and not affect the damage due to liquefaction (NIBS, 2004). Once the probabilities of exceeding the specified DS are estimated, a damage index d_m is evaluated, to quantify the structural losses as the ratio of cost of repair to cost of replacement taking values from 0: no damage (cost of repair equals 0) to 1: complete damage (cost of repair equals the cost of replacement). Regarding the port buildings, the estimated damage indices are weighted with respect to the built area and multiplied with the average replacement cost per m^2 (an assumption of 800 Euro/m^2 is made) to derive the mean repair costs values per built area (Table 2).

The spatial distribution of the estimated losses for buildings indicates that a non-negligible percentage of the port buildings is expected to suffer significant losses (higher than moderate). The median values of this percentage range from 7% for the design scenario (NL approach) to 37% for the 4975 years scenario I (EQL approach). This is to be expected taking into account that all buildings were constructed with low or no seismic code provisions. Among the considered building typologies, the RC structures appear to be less vulnerable compared to the steel and URM systems. The estimated losses are also significantly dependent on the analysis approach. In particular, the EQL approach is associated with higher damages and losses even for the design scenario, while for the NL approach the losses to the cranes, waterfronts and electric power substations are

expected solely for the 4975 scenario I. As shown in Table 2, the distribution of repair cost of port buildings is consistent with the distribution of the degree of structural loss.

Table 2. Mean repair costs of the port buildings

Scenario	Analysis type	Repair cost (Euro)
475 years	EQL	7710
	NL	5680
4975 years I	EQL	17880
	NL	8170
4975 years II	EQL	10080
	NL	5940

The systemic risk is assessed following the methodology presented in the previous section (PRA approach) taking again into account the interdependencies of specific components. It is observed that the EQL approach is associated with higher number of non-functional components for all considered seismic scenarios whereas for the NL approach non-functional components are present only for the 4975 years scenario I. The estimated PIs of the port are normalized to the respective value referring to non-seismic conditions (Table 3). As also evidenced by the estimated functionality state of each component, the port system is non-functional both in terms of TCaH and TCoH for the 4975 years scenario I. A 100% and 67% performance loss is estimated for the TCoH and TCaH respectively when considering the EQL approach for the 475 years and 4975 years II scenarios, while the port is fully functional when considering the NL approach both in terms of TCaH and TCoH for the latter scenarios. Further details regarding the scenario based risk assessment are provided in Pitilakis et al. (2016).

Table 3. Estimated normalized performance loss of the port system for TCaH and TCoH and comparison with risk objectives for the scenario based assessment.

Scenario	Analysis type	Performance loss ($1-PI/PI_{max}$)		Risk objectives			Stress test outcome	
		TCaH	TCoH	AA-A	A-B	B-C	TCaH	TCoH
475 years	EQL	0.67	1.00	0.10	0.30	0.50	Fail	Fail
	NL	0.00	0.00				Pass	Pass
4975 years I	EQL	1.00	1.00	0.30	0.50	0.70	Fail	Fail
	NL	1.00	1.00				Fail	Fail
4975 years II	EQL	0.67	1.00				Partly pass	Fail
	NL	0.00	0.00				Pass	Pass

DECISION PHASE

The Decision phase comprises different steps including (i) the comparison of the assessment results with the pre-defined risk objectives, (ii) disaggregation and/or sensitivity analysis to identify critical events and components and (iii) recommendation of risk mitigation measures to improve the performance of the port.

Risk objectives check

In the first step of the decision phase, the risk assessment results are compared with the defined risk objectives to check whether the port system passes, partially passes or fails the stress test and to define the grading system parameters for the next evaluation of the stress test since the performance of the CI or performance objectives can change over time (Esposito et al. 2017).

In Fig. 9 risk boundaries are plotted together with the MAF curves of the assessed performance loss. With reference to both bulk cargo and container terminals (TCaH, TCoH curves) the port obtains grade B, meaning that the risk is possibly unjustifiable and the CI partly passes this evaluation. The basis for redefinition of risk objectives in the next evaluation of stress test is the characteristic point of risk, which is defined as the point associated with the greatest risk above the ALARP region (blue and red dots for TCaH and TCoH curves respectively). These points are the farthest from the A-B boundary (blue line). The proposed grading system foresees the reduction of the boundary between grades B and C (red line) in the next stress test, which is equal to the amount of risk beyond the ALARP region assessed, represented in this application by the corresponding red dashed lines in case of the bulk cargo and cargo terminals. The plot in Fig. 10 (left panel) indicates that the CI receives grade AA (negligible risk), and as expected in this example application, passes the stress test for the tsunami hazard. Indicative scalar performance boundaries in terms of the normalized performance loss are shown in Table 3 together with the corresponding results of the scenario based assessment. It is seen that the CI may pass, partly pass or fail for the specific evaluation of the stress test (receiving grades AA, B and C respectively) depending on the selected seismic scenario, the analysis approach and the considered risk metric (TCaH, TCoH). It is noted that different grades can be derived from the probabilistic and scenario-based assessments varying between AA (for the scenario based and the probabilistic tsunami risk assessments) and C (for the scenario-based and probabilistic seismic risk assessments). It is also worth noting that the risk objectives and the time between successive stress tests should be defined by the CI authority and regulator. Since regulatory requirements do not yet exist for the port infrastructures, the boundaries need to rely on judgements.

CONCLUSIONS

The recently developed methodology ST@STREST for stress test of critical non-nuclear infrastructures was applied to the Port infrastructures of Thessaloniki, Greece exposed to different seismic hazards, i.e. ground shaking, liquefaction and tsunami. The vulnerability assessment of the infrastructures to the given hazards was performed using site and case specific or generic fragility functions. Specific risk metrics and objectives were defined related to the functionality of the port system and the structural losses. In the first level of the assessment phase, a risk-based assessment of each component was carried out for earthquake and tsunami hazards to check its performance. To accomplish that, the target (acceptable) probability of collapse implied by the code, stakeholders and decision-makers needs was pre-defined for each component. Then, a probabilistic risk analysis was conducted for the whole system separately for earthquake and tsunami hazards considering specific interdependencies between network and components. Site specific response and extreme seismic events were evaluated with a scenario-based risk analysis. In the decision phase, the estimated response was compared with predefined risk objectives in order to assess the performance of the CI and decide whether it passes, partly passes or fails the test for all possible events and to define how much the safety of the CI should be improved until the next periodical verification. Since no regulatory boundaries exist for port facilities, the risk objectives in this application were defined as continuous and scalar boundaries based on general judgment criteria for the probabilistic and scenario based system-wide risk assessment respectively. It has been shown that the port obtains grades B (the risk is possibly unjustifiable) and AA (negligible risk) for the PRA of earthquake and tsunami hazards respectively, meaning that the CI partly passes or passes this evaluation of the stress test. The comparison of the scenario based assessment response with the risk objectives indicates that the CI may pass, partly pass or fail for the specific evaluation of the stress test depending on the selected seismic scenario, the analysis approach and the considered risk metric. A next step of the decision phase is the identification of the critical components and events as well as the recommendation of risk mitigation strategies to upgrade the port operations and improve its resilience. Finally, in the Report phase, the outcome of the stress test (in terms of grades, critical events/components, guidelines for risk mitigation) is communicated to the port Authority. Based on the different outcomes of the stress test from the probabilistic and scenario-based assessments, it is up to the port Authority to decide to take specific measures to improve and upgrade or not the performance of the port.

ACKNOWLEDGEMENTS

The work reported in this paper was carried out in the framework of STREST project, funded by the European Community's Seventh Framework Programme (FP7/2007-2013) under grant agreement no. 603389. The

contribution of Volpe M, Tonini R, Romano F, Brizuela B, Piatanesi A, Basili R, Lorito S. (INGV, Italy) in the tsunami hazard analysis is also acknowledged.

REFERENCES

ABAQUS. Analysis User's Manual - version 6.10, 2012, Dassault Systèmes, SIMULIA Inc, USA.

Aki K. Space and Time Spectra of Stationary Stochastic Waves, with Special Reference to Microtremors. *Bull. Earthquake Res. Inst. Tokyo Univ*, 1957, 25: 415-457.

Akkar S, Bommer JJ. Empirical equations for the prediction of PGA, PGV and spectral accelerations in Europe, the Mediterranean and the Middle East. *Seismol Res Lett*, 2010, 81: 195–206.

Anastasiadis A, Raptakis D, Pitilakis K. Thessaloniki's detailed microzoning: subsurface structure as basis for site response analysis, *Pure and Applied Geophysics*, 2001, 158, 2597-2633.

Basili R, Tiberti MM, Kastelic V, Piatanesi A, Selva J, Lorito S. Integrating geologic fault data into tsunami hazard studies, *Natural Hazards and Earth System Sciences*, 2013, 13:1025-1050, DOI: 10.5194/nhess-13-1025-2013.

Bommer JJ, Acevedo AB. The use of real accelerograms as input to dynamic analysis, *Journal of Earthquake Engineering*, 2004, 8(1):43-91. DOI: 10.1080/13632460409350521.

Cornell C, Krawinkler H. Progress and challenges in seismic performance assessment. PEER News 2000, 3 (2).

Elgamal A, Yang Z, Lu J. Cyclic1D Seismic Ground Response Version 1.4, 2015, User's Manual, University of California, San Diego, Department of Structural Engineering.

EN 1998-1. Eurocode 8: Design of structures for earthquake resistance-Part 1: General rules, seismic actions and rules for buildings. CEN, Bruxelles, 2004.

Esposito S, Stojadinović B, Babič A, Dolšek M, Iqbal S, Selva J. Engineering risk-based methodology and grading system for stress testing of critical non-nuclear infrastructures (STREST Project), *16th World Conference on Earthquake Engineering*, 9-13 January 2017, Santiago, Chile.

Fajfar P, Dolšek M. A practice- oriented estimation of the failure probability of building structures. *Earthquake Engng Struct. Dyn*, 2012, 41 (3): 531–547.

Giardini D. et al. Seismic Hazard Harmonization in Europe (SHARE). Online Data Resource, http://portal.share-eu.org:8080/jetspeed/portal/, doi: 10.12686/SED-00000001-SHARE, 2013.

Gonzalez Vida JM et al. Tsunami-HySEA: a GPU based model for the Italian candidate tsunami service provider, *EGU General Assembly*, 2015, 12-17 April, Vienna, Austria, Abstract # EGU2015-13797.

Jayaram N, Baker JW. Correlation model of spatially distributed ground motion intensities. *Earthquake Engineering and Structural Dynamics*, 2009, 38 (15): 1687–1708.

Kakderi et al. Deliverable 4.2: Guidelines for performance and consequences assessment of geographically distributed, non-nuclear critical infrastructures exposed to multiple natural hazards. STREST project EC/FP7 (2007-2013), grant agreement No: 603389, 2015.

Kappos AJ, Panagiotopoulos C, Panagopoulos G, Panagopoulos El. WP4-Reinforced concrete buildings (Level I and II analysis), RISK-UE: An advanced approach to earthquake risk scenarios with applications to different European towns, 2003.

Kappos AJ, Panagopoulos G, Panagiotopoulos C, Penelis G. A hybrid method for the vulnerability assessment of R/C and URM buildings. *Bulletin of Earthquake Engineering*, 2006, 4:391-419.

Karafagka S, Fotopoulou S, Pitilakis K. Tsunami fragility curves for seaport structures, *1st International Conference on Natural Hazards & Infrastructure*, 28-30 June 2016, Chania, Greece.

Kottke AR, Rathje EM. Technical Manual for Strata. PEER Report 2008/10. University of California, Berkeley.

Kourkoulis R, Gelagoti F, Loli M, Gazetas G. Interplay of container port cranes and Quay-Walls during earthquake shaking, *Second European Conference on Earthquake Engineering and Seismology*, Istanbul, Aug. 25-29, 2014.

Lazar N, Dolšek M. Application of the risk-based seismic design procedure to a reinforced concrete frame building, *4th ECCOMAS Thematic Conference on Computational Methods in Structural Dynamics and Earthquake Engineering*, M. Papadrakakis, V. Papadopoulos, V. Plevris (eds.) Kos Island, Greece, 12–14 June 2013.

Lorito S, Selva J, Basili R, Romano F, Tiberti MM. Piatanesi A. Probabilistic hazard for seismically-induced tsunamis: accuracy and feasibility of inundation maps, *Geophys. J. Int.*, 2015, 200 (1): 574-588.

Marzocchi W, Taroni M, Selva J. Accounting for epistemic uncertainty in PSHA: logic tree and ensemble modeling, *Bulletin of the Seismological Society of America*, 2015, 105 (4), doi: 10.1785/0120140131.

Molinari I, Tonini R, Piatanesi A, Lorito S, Romano F, Melini D, Gonzalez Vida JM, Macias J, Castro M, de la Asuncion M. Fast evaluation of tsunami scenarios: uncertainty assessment for a Mediterranean Sea database, *submitted to NHESS* (under review), 2016.

National Institute of Building Sciences, NIBS. Direct physical damage—general building stock. HAZUS-MH Technical manual, Chapter 5. Federal Emergency Management Agency, Washington, D.C, 2004.

Papaioannou C. Seismic hazard scenarios-Probabilistic seismic hazard analysis, SRM-Life Project: Development of a global methodology for the vulnerability assessment and risk management of lifelines, infrastructures and critical facilities. Application to the metropolitan area of Thessaloniki (in greek), 2004.

Parsons T, Geist EL. Tsunami probability in the Caribbean region, *Pure appl. Geophys.*, 2009, 165: 2089–2116.

PIANC. Seismic Design Guidelines for Port Structures, International Navigation Association, Balkema, 474 p, 2001.

Pitilakis K, Crowley H., Kaynia A (Eds). SYNER-G: Typology definition and fragility functions for physical elements at seismic risk. Buildings, lifelines, transportation networks and critical facilities. Geotechnical, *Geological and Earthquake Engineering*, 2014a, 27, Springer, Netherlands.

Pitilakis K, Franchin P, Khazai B, Wenzel H. (Eds). SYNER-G: Systemic seismic vulnerability and risk assessment of complex urban, utility, lifeline systems and critical facilities. Methodology and applications. *Geotechnical, Geological and Earthquake Engineering*, 2014b, 31, Springer, Netherlands.

Pitilakis K. et al. Deliverable D6.1: Integrated report detailing analyses, results and proposed hierarchical set of stress tests for the six CIs covered in STREST, STREST project: Harmonized approach to stress tests for critical infrastructures against natural hazards, 2016.

Selva J, Tonini R, Molinari I, Tiberti MM, Romano F, Grezio A, Melini D, Piatanesi A, Basili R, Lorito S Quantification of source uncertainties in Seismic Probabilistic Tsunami Hazard Analysis (SPTHA), *Geophys. J. Int.*, 2016a, doi:10.1093/gji/ggw107.

Selva J, Tonini R, Romano F, Volpe M, Brizuela B, Piatanesi A, Basili R, Lorito S. From regional to site specific SPTHA through inundation simulations: a case study for three test sites in Central Mediterranean, EGU General Assembly 2016b, 17-22 April, Vienna, Austria, Abstract #EGU2016-16988.

Selva, J. Long-term multi-risk assessment: statistical treatment of interaction among risks. Natural Hazards, 2013, 67 (2): 701-722.

Silva V, Crowley H, Bazzuro P. Risk-targeted hazard maps for Europe. Second European Conference on Earthquake Engineering and Seismology, Istanbul, 24-29 August, 2014, Turkey.

Smerzini C, Pitilakis K, Hasmemi K, submitted. Evaluation of earthquake ground motion and site effects in the Thessaloniki urban area by 3D finite-fault numerical simulations, *Bulletin of Earthquake Engineering*, 2016.

SRMLIFE. Development of a global methodology for the vulnerability assessment and risk management of lifelines, infrastructures and critical facilities. Application to the metropolitan area of Thessaloniki. Research project, General Secretariat for Research and Technology, Greece (in greek), 2007.

Salzano et al. Deliverable D4.1: Guidelines for performance and consequences assessment of single-site, high-risk, non-nuclear critical infrastructures exposed to multiple natural hazards, covered in STREST (AUTH contribution), STREST project: Harmonized approach to stress tests for critical infrastructures against natural hazards, 2015.

Toro GR. Probablistic models of site velocity profiles for generic and site-specific ground-motion amplification studies. Upton, New York: Brookhaven National Laboratory, 1995.

UPGRADE. Technical reports with the calculation results of the vulnerability of specific Greek port facilities (in Greek). Deliverable 8.2, 2015, Research project: Contemporary Evaluation Methodology of Seismic Vulnerability and Upgrade of Port Facilities, http://excellence.minedu.gov.gr/thales/en/thalesprojects/380174

Volpe M, Selva J, Tonini R, Romano F, Brizuela B, Piatanesi A, Basili R, Lorito S, in prep: From regional to site specific SPTHA through inundation simulations: a case study for Milazzo (Italy) and Thessaloniki (Greece).

Weatherill G, Esposito S, Iervolino I, Franchin P, Cavalieri F. Framework for seismic hazard analysis of spatially distributed systems, in: K. Pitilakis et al. (eds). Systemic seismic vulnerability and risk assessment of complex urban, utility, lifeline systems and critical facilities. Methodology and applications. 2014, Springer, Netherlands, 57-88.